Robust and Passive Model Order Reduction for Circuits Containing Susceptance Elements†

Hui Zheng and Lawrence T. Pileggi
Carnegie Mellon University, Department of Electrical and Computer Engineering
5000 Forbes Avenue
Pittsburgh, PA 15213
{hzheng, pileggi}@ece.cmu.edu

ABSTRACT

Numerous approaches have been proposed to address the overwhelming modeling problems that result from the emergence of magnetic coupling as a dominant performance factor for ICs and packaging. Firstly, model order reduction (MOR) methods have been extended to robustly capture very high frequency behaviors for large RLC systems via methods such as PRIMA[8] with guaranteed passivity. In addition, new models of the magnetic couplings in terms of susceptance (inverse of inductance) have shown great promise for robust sparsification of otherwise intractable inductance coupling-matrix problems[3-5]. However, model order reduction via PRIMA for circuits that include susceptance elements does not guarantee passivity. Moreover, susceptance elements are incompatible with the path tracing algorithms that provide the fundamental runtime efficiency of RICE [10]. In this paper a novel MOR algorithm, SMOR, is proposed as an extension of ENOR [11] which exploits the matrix properties of susceptance-based circuits for runtime efficiency, and provides for a numerically stable, provably passive MOR using a new orthonormalization strategy.

1 INTRODUCTION

Due to the increasing operating frequencies and larger sizes of on-chip and off-chip interconnect systems, it has become a daunting task to perform signal integrity analyses for systems containing hundreds of thousands of conductors while accounting for all of the capacitive and inductive couplings. Among the challenges, the extraction, modeling and simulation of the magnetic couplings has been the focus of research due to the following difficulties. First, when the return paths can not be determined prior to the extraction and simulation of an interconnect system, a partial inductance matrix must be formed which can be extremely large and dense [1]. Since arbitrarily discarding small terms may render the circuit model unstable, special sparsification strategies, most notably the shift-and-truncate technique in [2], have been devised to preserve the positive definiteness of the partial inductance matrix. This sparsification is limited, however, if the shell has to be chosen to be large enough to guarantee accuracy.

Very recently the concept of susceptance has emerged as an alternative way for modeling magnetic couplings [3, 4]. As the inverse of a partial inductance matrix, a susceptance matrix has properties similar to a capacitance matrix (the inverse of a potential matrix). Firstly, susceptance inherently provides a shielding effect whereby the mutual susceptance terms drop off much faster than the mutual inductance terms with distance. Secondly, a susceptance matrix is diagonally dominant which guarantees its positive definiteness under simple truncation. As a result, window-based extraction can be used to build a sparse susceptance matrix by piecing together the localized extraction window results. Furthermore, in [5] it was recently shown that susceptance-based modeling and simulation are superior to inductance-based approaches due to the superior sparsity of the susceptance matrix and the inherent symmetric positive definite formulation which enables fast matrix solutions in the inner-most-loops during transient simulation.

Unrelated, but equally important, various model order reduction (MOR) algorithms, such as AWE [6], PVL [7], and PRIMA [8], have been developed during the past fifteen years to also address the interconnect complexity problem. These MOR approaches primarily serve two functions: 1) reduce the circuit size so that efficient time-domain analysis can be performed; 2) accurately extract frequency-domain characteristics by identifying the dominant pole information. The emergence of Krylov subspace methods [7] has facilitated the application of MOR to large, coupled, RLC systems. With the emergence of couplings and the need to model large N-port problems, methods such as PRIMA have provided reliable MOR with similar accuracy and guaranteed passivity [9].

Even with susceptance to control the complexity of modeling the magnetic couplings, MOR is desirable to accommodate the overall complexity of the complete RCS (S representing susceptance) system. However, we will show that the path-tracing technique [10] that enables fast calculation of moments or Krylov vectors in RICE can no longer be directly applied for mutual susceptance elements. Furthermore, we will demonstrate that applying PRIMA directly to the RCS circuit equations does not guarantee passivity.

In [11], Sheehan proposed ENOR, a MOR algorithm that exploits the symmetric positive definite formulation brought by the inverse of the inductance matrix. This algorithm provides an elegant solution for the aforementioned problems associated with RCS circuits by calculating only the node voltage moment vectors. However, as we will show in this paper, two problems prevent ENOR from challenging other popular MOR algorithms for RCL circuits. Firstly, the numerical procedure used in ENOR is not robust enough to generate accurate high-order reduced models; secondly, the reduced-order models generated by ENOR can only be used for time-domain simulation, and no frequency-domain characteristics, such as dominant poles and transfer functions, can be easily extracted.

To address the first problem in ENOR, we propose a new orthonormalization strategy which can greatly improve the numerical robustness without increasing the computational complexity. A detailed description of this procedure is described in Section 3. In Section 4 we propose a novel MOR algorithm for RCS circuits, SMOR, that can generate extended moment vectors including susceptance currents while preserving the efficiency by way of solving symmetric positive definite equations. In addition, the procedure of generating the transformation matrix can be made very robust through an orthonormalization strategy similar to that described in Section 3. As in PRIMA, poles and transfer functions can be readily calculated from the reduced-order models gener-

†This work was supported by Semiconductor Research Corporation (SRC) under contract 2000-TJ-778.

0-7803-7607-2/02/$17.00 ©2002 IEEE

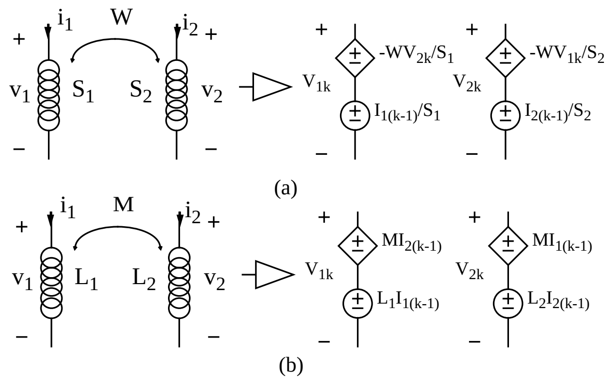

Fig. 1. Comparison of DC circuits for Mutual Susceptance and Mutual Inductance

ated by SMOR. Section 5 shows some experimental results which validate the accuracy and efficacy of our new algorithms. Finally, some conclusions are drawn in Section 6.

2 BACKGROUND

Since a susceptance matrix is the inverse of an inductance matrix, the differential system matrix equations that describe an RCS circuit can be directly stated as:

$$\begin{bmatrix} G & A_S \\ -SA_S^T & 0 \end{bmatrix}\begin{bmatrix} V_n \\ I_S \end{bmatrix} + \begin{bmatrix} C & 0 \\ 0 & I \end{bmatrix}\begin{bmatrix} \dot{V}_n \\ \dot{I}_S \end{bmatrix} = \begin{bmatrix} -A_{CS} I_{CS} \\ 0 \end{bmatrix} \qquad (1)$$

where G and C present the contribution from resistances/conductances and capacitances; A_S and A_{CS} are incidence matrices for susceptances and current sources; V_n and I_S are the node voltage vector and the susceptance current vector; and S is the susceptance matrix.

Applying the Laplace transform to both sides of (1) and Taylor expanding the state vectors around $s = 0$:

$$\begin{bmatrix} G & A_S \\ -SA_S^T & 0 \end{bmatrix}\begin{bmatrix} X_0 + sX_1 + \dots \\ I_0 + sI_1 + \dots \end{bmatrix} + s\begin{bmatrix} C & 0 \\ 0 & I \end{bmatrix}\begin{bmatrix} X_0 + sX_1 + \dots \\ I_0 + sI_1 + \dots \end{bmatrix} = \begin{bmatrix} B \\ 0 \end{bmatrix}(J_0 + sJ_1 + \dots) \qquad (2)$$

Where for notational simplicity, we designate $X = V_n$, $I = I_S$, $B = -A_{CS}$, and $J = I_{CS}$. Also, since impulse responses are normally required for moment matching, J_k is 0 for $k > 0$. To facilitate matching of the moments in (2), moment generation can be performed based on the following recurrence relation:

$$\begin{bmatrix} G & A_S \\ -SA_S^T & 0 \end{bmatrix}\begin{bmatrix} X_k \\ I_k \end{bmatrix} = -\begin{bmatrix} C & 0 \\ 0 & I \end{bmatrix}\begin{bmatrix} X_{k-1} \\ I_{k-1} \end{bmatrix} \text{ for } k > 0 \text{ and } \begin{bmatrix} G & A_S \\ -SA_S^T & 0 \end{bmatrix}\begin{bmatrix} X_0 \\ I_0 \end{bmatrix} = \begin{bmatrix} BJ_0 \\ 0 \end{bmatrix} \qquad (3)$$

For model order reduction of RCL circuits, a recurrence relation similar to (3) can be used to generate moments. While the straightforward way is to solve the linear system using matrix techniques, the path-tracing technique [10], which provides the fundamental runtime efficiency of RICE, can solve the DC circuit representation for interconnect circuits with extreme efficiency. However, the path-tracing technique is not applicable to the susceptance-based moment generation, which can be established in the following simple arguments. Suppose the branch constitutive relations for a pair of coupled susceptances are:

$$\frac{di_1}{dt} = S_1 v_1 + W v_2 \qquad (4)$$
$$\frac{di_2}{dt} = W v_1 + S_2 v_2$$

where W represents the mutual susceptance. The recurrence relation of (4) for moments expanded around $s = 0$ is:

$$V_{1k} = \frac{1}{S_1} I_{1(k-1)} - \frac{W}{S_1} V_{2k} \qquad (5)$$
$$V_{2k} = \frac{1}{S_2} I_{2(k-1)} - \frac{W}{S_2} V_{1k}$$

which means that if the susceptances are replaced by concatenations of voltage sources and voltage controlled voltage sources (Fig. 1 (a)) in the DC circuit for moment generation, the present susceptance voltage moments can not be determined solely from the previous susceptance current moments. This property fundamentally prevents the use of path-tracing, since path-tracing requires that all capacitor current moments and susceptance voltage moments be known prior to the DC circuit solution. In contrast, in inductance-based formulations, the present inductor voltage moments can be calculated from the previous inductor current moments, as shown in Fig. 1 (b).

One may think the remedy to this problem is to expand the Laplace-domain responses around $s = \infty$, i.e. $X(s) = X_0 + \frac{1}{s}X_{-1} + \frac{1}{s^2}X_{-2} + \dots$. Then, the recurrence relation in (5) can be converted into:

$$I_{1(-k)} = S_1 V_{1(-(k-1))} + W V_{2(-(k-1))} \qquad (6)$$
$$I_{2(-k)} = W V_{1(-(k-1))} + S_2 V_{2(-(k-1))}$$

Consequently, if the susceptances are replaced by concatenations of current sources and voltage controlled current sources, the present susceptance current moments can be readily computed from the previous susceptance voltage moments. However, for self-consistence in the generation of moments, a potential matrix, instead of a capacitance matrix, must be used for the capacitors to be represented as voltage sources in the DC circuit. It is well-known that a potential matrix, like an inductance matrix, is very hard to sparsify, which in fact defeats the advantage of using susceptances in place of inductances.

Even more importantly, if one opts to use matrix techniques to solve the equations in (3), there still exists the problem that the reduced-order system obtained through PRIMA-like methods is not necessarily passive. As detailed in [8], preservation of passivity requires that the matrix $D + D^T$ be a nonnegative matrix when D is the matrix in front of the undifferentiated state vector in the differential system formulation. In the case that $D = \begin{bmatrix} G & A_S \\ -SA_S^T & 0 \end{bmatrix}$ as in (1), this condition can not be satisfied.

In [11], Sheehan proposed ENOR, a MOR algorithm, which provides an elegant solution for the aforementioned problems. The following is a brief description of the ENOR algorithm. For more details, please refer to the original paper [11].

In ENOR, a Laplace-domain nodal formulation, instead of the MNA formulation in (2), is used:

$$\left(Cs + G + \frac{\Gamma}{s}\right)X(s) = BJ(s) \qquad (7)$$

where $\Gamma = A_S S A_S^T$. Then, the basic procedure for model order reduction is to find an orthonormal basis V for node voltage moment vectors up to a certain order and perform an orthogonal projection on this system, which is similar to what is done in PRIMA. The reduced-order system has the form:

$$\left(\tilde{C}s + \tilde{G} + \frac{\tilde{\Gamma}}{s}\right)\tilde{X}(s) = \tilde{B}J(s) \qquad (8)$$

where $\tilde{C} = V^T C V$, $\tilde{G} = V^T G V$, $\tilde{\Gamma} = V^T \Gamma V$ and $\tilde{B} = V^T B$.

What is interesting is how the moment vectors are generated in ENOR. After performing a variable substitution $z = \frac{-1}{s_0}(s - s_0)$ to (7) as shown in the paper, a recurrence relation can be obtained for moment generation:

$$\left(Cs_0 + G + \frac{\Gamma}{s_0}\right)X_k = Cs_0 X_{k-1} - \frac{\Gamma}{s_0} Y_{k-1} + BJ_k \qquad (9)$$

$$Y_k = X_k + Y_{k-1} \quad (10)$$

$$X_{-1} = Y_{-1} = 0 \quad (11)$$

Note that the matrix on the left side of (9) is symmetric positive definite (s.p.d.) which is casually stated in Sheehan's paper. A more rigorous proof of this property for the RCS formulation can be found in [5]. This property is very advantageous for fast direct sparse matrix solutions, since no pivoting is required and powerful ordering algorithms can be employed prior to the actual factorization in order to reduce potential fill-ins [13]. As a result, the efficiency achieved through solving a s.p.d. system can approach that of path-tracing.

The generated X vectors in (9) are actually the scaled node voltage moments expanded about the frequency s_0. It is worth noting that frequency shifting is essential for establishing the recurrence relation in (9), and the computational cost does not change with regard to the value of s_0. However, frequency shifting is detrimental to the path-tracing technique, since extra resistors and current controlled voltage sources corresponding to the shift frequency s_0 have to be added which slows down path tracing significantly. Therefore, for the cases in which frequency shifting must be applied in order to get accurate moments around certain high frequencies [12], ENOR and the algorithms presented in this paper can be computationally more efficient than the MOR algorithms using frequency-shifted path tracing.

In the algorithm shown in the ENOR paper, an orthonormalization procedure is designed in order to gain better numerical stability. However, since only the X vectors are actually orthonormalized, the Y vectors, though computed in synch with X vectors to keep the spanned subspace intact, can grow rapidly in magnitude and cause numerical inaccuracy when the order is high. We address this problem with our orthonormalization strategy in Section 3.

Another disadvantage with ENOR is that the reduced-order system can only be simulated to get the time-domain response, and it is impractical to calculate the poles and the frequency-domain responses of the reduced-order system due to the difficulty of inverting the matrix in (8). The algorithm SMOR presented in Section 4 provides a solution to this problem.

3 NEW ORTHONORMALIZATION STRATEGY

Since it is observed that the numerical problem with ENOR lies in the Y vectors, our first step is to get rid of these vectors. It can derived from (10) that:

$$Y_k = \sum_{i=0}^{k} X_i \quad (12)$$

By substituting (12) into (9), we get a new recurrence relation:

$$X_k = PX_{k-1} + Q\sum_{i=0}^{k-1} X_i \text{ for } k > 0 \quad (13)$$

$$X_{-1} = 0 \quad X_0 = \left(Cs_0 + G + \frac{\Gamma}{s_0}\right)^{-1} B \quad (14)$$

where $P = \left(Cs_0 + G + \frac{\Gamma}{s_0}\right)^{-1} Cs_0$ and $Q = -\left(Cs_0 + G + \frac{\Gamma}{s_0}\right)^{-1} \frac{\Gamma}{s_0}$.

It can be proven by induction that $span(X_0, X_1, X_2, \ldots X_k)$ is a subspace of a generalized Krylov subspace $\kappa(P, Q, X_0, k)$, the definition of which is:

$\kappa(P, Q, X_0, k) = span(P_0(P, Q)X_0, \ldots, P_k(P, Q)X_0)$

$P_i(P, Q)$ is the space spanned by all the homogeneous polynomials of P and Q of order i. It is interesting to point out that this concept of generalized Krylov subspace has been used for numerical analysis of eigenvalue problems [14]. Now it also finds its way into model order reduction, just like Krylov subspace theory has been the foundation for many MOR algorithms for RCL circuits, such as PVL [7] and PRIMA [8].

Algorithm ImpENOR

$X_{-1} = 0$

$X_0 = \left(Cs_0 + G + \frac{\Gamma}{s_0}\right)^{-1} B$ and $X_0 = orth(X_0)$

$V = X_0$

for k= 1:q/n

  Set $T = Cs_0 X_{k-1} - \frac{\Gamma}{s_0}(X_{k-1} + X_{k-2})$

  Solve $\left(Cs_0 + G + \frac{\Gamma}{s_0}\right)X_k = T$

  Orthonormalize X_k against $X_0, X_1, \ldots X_{k-1}$ and itself

  $V = [V\ X_k]$

end

Fig. 2. Improved ENOR Algorithm

However, the summation in the recurrence relation still presents a numerical problem, since errors can be accumulated. This leads to our next step, namely simplification of the recurrence relation:

$$X'_k = PX'_{k-1} + QX'_{k-1} + QX'_{k-2} \text{ for } k > 0 \quad (15)$$

The rationale behind this simplification is that it can be again proven by induction that $span(X'_0, X'_1, X'_2, \ldots X'_k)$ is a subspace of the same generalized Krylov subspace $\kappa(P, Q, X_0, k)$. Moreover, our later experimental results demonstrate that $span(X'_0, X'_1, X'_2, \ldots X'_k)$ presents a very close approximation of $span(X_0, X_1, X_2, \ldots X_k)$.

More importantly, the recurrence relation in (15) is more amenable to orthonormalization, a powerful numerical technique which provides superb numerical stability. It can also be proven that orthonormalization leaves $span(X'_0, X'_1, X'_2, \ldots X'_k)$ intact, which is critical for model order reduction, since it is the subspace, not the identity of the individual vectors, that determines the eigenvalues/poles of the reduced-order system.

A numerically improved ENOR for generating the transformation matrix V is presented in Fig. 2. Note that since there is no additional processing for Y vectors, the computational cost is reduced.

4 SMOR: ROBUST AND PASSIVE MODEL ORDER REDUCTION FOR RCS CIRCUITS

The main reason that ENOR fails to provide frequency-domain information is that its formulation in (7) is a second-order system instead of a first-order system equivalent to those used in MOR algorithms for RCL circuits. Therefore, in order to use the first-order formulation in (1), extended moment vectors including susceptance currents should be generated. The following derives a new recurrence relation which can facilitate efficient generation of extended moment vectors.

Note that the current vector for susceptances can be computed from node voltage vector, which in Laplace-domain is:

$$I(s) = \frac{SA_S{}^T}{s} X(s) \quad (16)$$

Performing a same variable substitution as that in the ENOR paper yields:

$$I(z) = \frac{SA_S{}^T}{s} X(z) = \frac{SA_S{}^T}{s_0} Y(z) \quad (17)$$

which can be represented in terms of moments as:

$$I_k = \frac{SA_S{}^T}{s_0} Y_k = W \sum_{i=0}^{k} X_i = I_{k-1} + WX_k \tag{18}$$

where $W = \frac{SA_S{}^T}{s_0}$.

Combining the relations in (13) and (18), we get a recurrence relation for the extended moment vectors:

$$M_k = \begin{bmatrix} X_k \\ I_k \end{bmatrix} = UM_{k-1} + V\sum_{i=0}^{k-1} M_i \tag{19}$$

$$M_{-1} = 0 \,,\; M_0 = \begin{bmatrix} \left(Cs_0 + G + \frac{\Gamma}{s_0}\right)^{-1} B \\ W\left(Cs_0 + G + \frac{\Gamma}{s_0}\right)^{-1} B \end{bmatrix} \tag{20}$$

where $U = \begin{bmatrix} P & 0 \\ WP & I \end{bmatrix}$ and $V = \begin{bmatrix} Q & 0 \\ WQ & 0 \end{bmatrix}$. The resulting M vectors are actually the scaled moment vectors of the original system expanded about the frequency s_0, which can be otherwise computed through the moment generation method by solving the equations in (3). But our new recurrence relation preserved the feature in ENOR that only one factorization of a symmetric positive definite matrix is required for moment generation, which can be seen more clearly in Fig. 3.

More importantly, noticing the striking similarity between the recurrence relations in (13) and (19), we can apply the same simplification and orthonormalization strategies discussed in Section 3 for numerically robust generation of an orthonormal basis for the extended moment vectors. After the orthonormal basis is found, a similar procedure as in PRIMA can be used to reduce the system and calculate the poles and residues.

However, as is discussed in Section 2, model order reduction to the system formulated in (1) does not guarantee passivity. A remedy to this problem is the following. Given a Cholesky decomposition of the susceptance matrix $S = R^T R$, which can be computed during the window-based extraction on the fly [3, 4] (R is upper triangular and has the same sparsity structure as S), the original system can be reformulated as:

$$\begin{bmatrix} G & A_S R^T \\ -RA_S^T & 0 \end{bmatrix} \begin{bmatrix} V_n \\ I_m \end{bmatrix} + \begin{bmatrix} C & 0 \\ 0 & I \end{bmatrix} \begin{bmatrix} \dot{V}_n \\ \dot{I}_m \end{bmatrix} = \begin{bmatrix} BJ \\ 0 \end{bmatrix} \tag{21}$$

where $I_m = (R^T)^{-1} I_S$. This vector transformation, however, does not present a problem, since applying this transformation to (18) we can obtain:

$$I_{mk} = (R^T)^{-1} I_k = \frac{(R^T)^{-1} SA_S{}^T}{s_0} Y_k = \frac{RA_S{}^T}{s_0} Y_k \tag{22}$$

Obviously, when $D = \begin{bmatrix} G & A_S R^T \\ -RA_S^T & 0 \end{bmatrix}$, the matrix $D + D^T$ is a nonnegative matrix, which satisfies the condition required for preservation of passivity [8]. The only thing we need to update for the recurrence relation in (19) is $W = \frac{RA_S{}^T}{s_0}$. For notational simplicity, we designate $H = \begin{bmatrix} G & A_S R^T \\ -RA_S^T & 0 \end{bmatrix}$ and $J = \begin{bmatrix} C & 0 \\ 0 & I \end{bmatrix}$.

Assembling all those important elements discussed above, the complete flow for our passive model order reduction algorithm SMOR is shown in Fig. 3, where q is the desired order, N is the number of ports, nn is the number of nodes and ns is the number of susceptances.

Algorithm SMOR

Build all the matrices required in (7) and (21), and choose an s_0.

$M_{-1} = 0$

$X_0 = \left(Cs_0 + G + \frac{\Gamma}{s_0}\right)^{-1} B$, $M_0 = \begin{bmatrix} X_0 \\ \frac{RA_S{}^T}{s_0} X_0 \end{bmatrix}$, $(M_0, T) = qr(M_0)$

If $\frac{q}{N}$ is not an integer, set $n = \left\lfloor \frac{q}{N} \right\rfloor + 1$, else set $n = \frac{q}{N}$

for $k = 1, 2, \ldots, n$

  Set $X_{k-1} = M_{k-1}(1\ldots nn)$ $X_{k-2} = M_{k-2}(1\ldots nn)$

  Set $I_{k-1} = M_{k-1}(nn+1\ldots nn+ns)$

  $T = Cs_0 X_{k-1} - \frac{\Gamma}{s_0}(X_{k-1} + X_{k-2})$

  Solve $\left(Cs_0 + G + \frac{\Gamma}{s_0}\right) X_k = T$

  $I_k = \frac{RA_S{}^T}{s_0} X_k + I_{k-1}$, $M_k = \begin{bmatrix} X_k \\ I_k \end{bmatrix}$

  orthonormalize M_k against $M_0, M_1, \ldots M_{k-1}$ and itself

end

Set $V = \begin{bmatrix} M_0 & M_1 & \ldots & M_{n-1} \end{bmatrix}$ and truncate V so that it has q columns.

Compute $\tilde{H} = V^T H V$ and $\tilde{J} = V^T J V$

Find eigendecomposition of $\tilde{H}^{-1}\tilde{J}$: $\tilde{H}^{-1}\tilde{J} = F \Lambda F^{-1}$

$\Lambda = diag(\lambda_1, \lambda_2, \ldots, \lambda_q)$

To find poles and residues for $Z_{i,j}(s)$:

  Solve $\tilde{H} w = V^T b_j$ for w

  Set $\mu = F^T V^T l_i$ and $\nu = F^{-1} w$

  $Z_{i,j}(s) = \sum_{i=1}^{q} \frac{\mu_i \nu_i}{1 + s\lambda_i}$

Fig. 3. SMOR Algorithm

In order to perform complete time-domain circuit simulation, the reduced-order model generated by SMOR can be combined with nonlinear elements through either direct stamping and realization or Z-parameter based simulation, as discussed in [8].

5 EXPERIMENTAL RESULTS

To demonstrate and validate the accuracy and efficacy of our new MOR algorithms, we have implemented the original ENOR algorithm (OrigENOR), our improved ENOR algorithm (ImpENOR), and our SMOR algorithm in Matlab [15]. All the following experiments are performed on a Sun Ultra 5 model 360 machine.

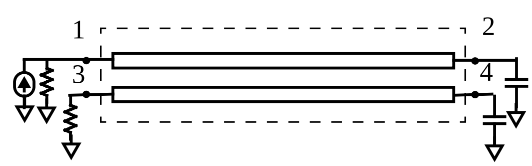

Fig. 4. Coupled 2-bit Bus

The example circuit used in our initial experiments is a capacitively and inductively coupled 2-bit bus, as shown in Fig. 4. This bus has the length of 3000 microns and is modeled with 60 coupled RSC sections. Each line has the width of 1 micron and height of 1 micron and the

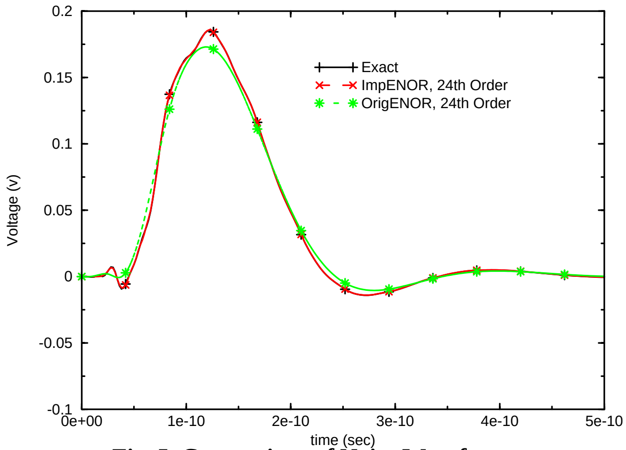

Fig. 5. Comparison of Noise Waveforms

spacing between the two lines is 1 micron. The capacitance and susceptance values are not artificial, since they are extracted by a full 3D field solution tool using a windowing technique [3, 4]. At the near ends of the two lines, one line is driven by the Norton equivalent of a driver for fitting into the NA formulation, while the other line is quiet and only connected to the ground through a resistor. Both lines have capacitive loads at their far ends.

To demonstrate the accuracy gain from our orthonormalization strategy in the improved ENOR, we compare the noise responses at port 4 from three different approaches: 1) transient susceptance-based simulation of the original system (Exact), which has also been implemented in Matlab; 2) ImpENOR; 3) OrigENOR. All the noise waveforms are shown in Fig. 5. While ImpENOR produces a waveform which is indistinguishable from the exact one, OrigENOR underestimates the noise peak slightly.

The comparison of runtime for transient simulation of the original and reduce-order systems is tabulated in Table 1. For this relatively small circuit (242 nodes), the MOR can speed up the simulation by about 30 times. For larger circuits, more significant speed-ups are expected, which will be very useful for simulation of enormous RCS circuits extracted to model electronic system packaging [5].

Exact	ImpENOR (24th Order)
29.37 sec	0.90 sec

Table 1. Runtime Saving from MOR

We have also applied the SMOR algorithm to this simple circuit example. Since SMOR generates almost the same time-domain responses as ImpENOR, we focus on demonstrating SMOR's ability to capture frequency-domain characteristics. We choose to look at the frequency response of the input impedance ($z_{11}(s)$) at port 1. To get the exact response, an eigen-solving procedure, similar to the one in SMOR (Fig. 3), is used, except for that the original MNA matrices are in the place of the transformed matrices. Fig. 6 shows the comparison of the frequency responses from SMOR using 48 poles and 72 poles against the exact response. While the reduced 72th-order response is almost indistinguishable from the exact response up to 80 GHz, even the less accurate model with 48 poles can match up to 60 GHz.

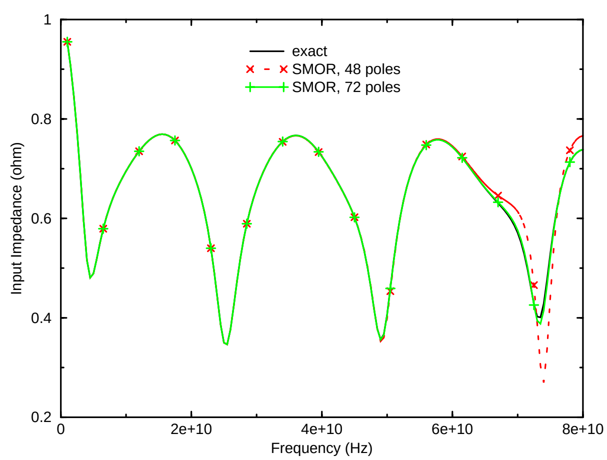

Fig. 6. Comparison of Frequency Responses

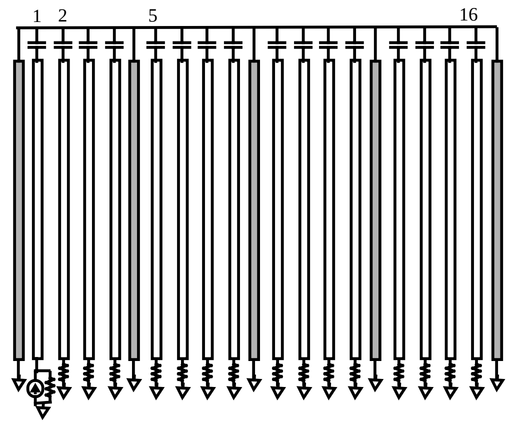

Fig. 7. 16-bit Bus with 5 Ground Returns

As a test of our algorithm on larger circuits we created the example shown in Fig. 7, which represents a 16-bit bus (white) with 5 periodic ground returns (grey). All 21 wires are 4000-micron long, 1-micron wide and 1-micron thick with a spacing of 1 micron, representative of a long signal path for an IC package. Each wire is modeled by 40 RCS sections, and the coupling capacitances and mutual susceptances among those sections are modeled via a windowing technique. There are 1702 nodes and 5803 elements in the extracted circuit. The circuit model also includes 50 ohm resistors connected to the near end of each bit line, load capacitance at the far end of each line of 2 ff. Bit 1 line is driven by a ramp current with a 10 ps risetime and an driver impedance (Norton equivalent admittance) of 50 ohms.

We compared a susceptance-based transient simulation using a circuit simulator that was modified to include susceptances with the response obtained via SMOR. We compared the voltage waveforms at the far end of the switching bit 1 line and the noise responses at the far end of the bit 5 line, which are shown in Fig. 8 and Fig. 9 respectively. While it is observed that more oscillatory noise waveforms generally requires higher orders of approximation, from the results shown it is evident that SMOR is capable of generating very accurate high order approximations for such systems.

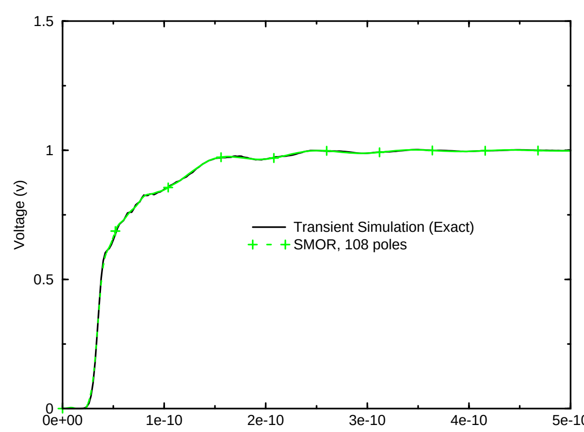

Fig. 8. Waveforms at Far End of Bit 1 Line

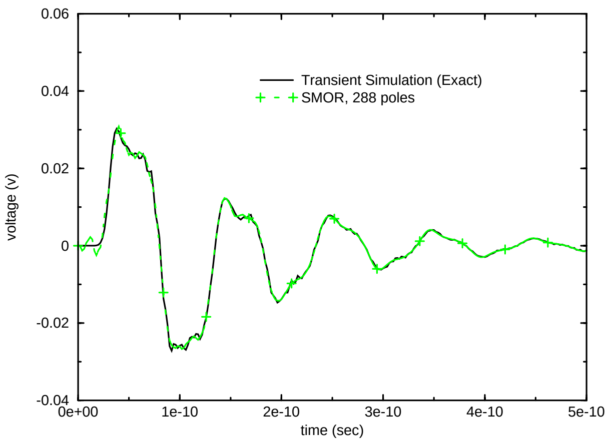

Fig. 9. Waveforms at Far End of Bit 5 Line

6 CONCLUSIONS

In this paper we investigated various issues associated with model order reduction for RCS (resistance-capacitance-susceptance) circuits. Based on the investigation, we propose a novel susceptance-based MOR algorithm SMOR. SMOR not only seamlessly incorporates the two important features associated with susceptance, namely sparsity and symmetric positive definite formulation, but also possesses the desired properties for a MOR algorithm, namely numerical stability through a new orthonormalization strategy and preservation of passivity. Like PRIMA, SMOR is able to provide frequency-domain information, and is easy to implement. Some experimental results demonstrate the efficacy and accuracy of SMOR.

7 REFERENCES

[1] D. Ling and A. Ruehli, *Circuit Analysis, Simulation and Design -- Advances in CAD for VLSI, Vol. 3, Part II*, Chapter 11, Elsevier Science Publisher B. V., North-Holland, 1987

[2] B. Krauter and L. Pileggi, "Generating Sparse Partial Inductance Matrices with Guaranteed Stability," IEEE/ACM Proc. ICCAD, pp. 45-52, Nov. 1995.

[3] M. Beattie and L. Pileggi, "Efficient Inductance Extraction via Windowing," IEEE/ACM Proc. 2001 DATE, pp. 430-436, March, 2001

[4] A. Devgan, H. Ji, and W. Dai., "How to Efficiently Capture On-Chip Inductance Effects: Introducing a New Circuit Element K," IEEE/ACM Proc. ICCAD, pp. 150-155, Nov. 2000

[5] H. Zheng, et. al. "Window-based Susceptance Models for Large-Scale RLC Circuit Analyses," IEEE/ACM Proc. 2002 DATE, pp. 628 - 633, March, 2002

[6] L. T. Pillage and R. A. Rohrer, "Asymptotic Waveform Evaluation for timing analysis," IEEE Trans. on CAD, vol 9, no 4, pp. 352-366, Apr. 1990

[7] P. Feldmann and R. W. Freund, "Efficient Linear Circuit Analysis by Padé Approximation via the Lanczos Process," IEEE Trans. on CAD, vol. 14, pp. 639-49, May 1995

[8] A. Odabasioglu, M. Celik and L. T. Pileggi, "PRIMA: Passive Reduced-Order Interconnect Macromodeling Algorithm," IEEE Trans. on CAD, vol. 17, no. 8, pp. 645-654, August 1998

[9] A. Odabasioglu, *PRIMA: Passive Reduced Order Interconnect Macromodeling Algorithm*, Ph.D. thesis, Carnegie Mellon University, September, 1999.

[10] C. L. Ratzlaff and L. T. Pillage, "RICE: Rapid Interconnect Circuit Evaluation Using AWE," IEEE Trans. on CAD, vol. 13, no. 6, pp. 763-776, Jun. 1994

[11] B. N. Sheehan, "ENOR: Model Order Reduction of RLC Circuits Using Nodal Equations for Efficient Factorization," in IEEE/ACM Proc. 36th DAC, pp. 17-21, June 1999

[12] M. Celik, L. Pileggi, and A. Odabasioglu, *IC Interconnect Analysis*, Kluwer Academic Publishers, 2002.

[13] A. George and J. Liu, *Computer Solution of Large Sparse Positive Definite Systems*, Prentice-Hall Inc., 1981

[14] T. Zhang, G.H. Golub, and K.H. Law. "Eigenvalue Perturbation and Generalized Krylov Subspace Method," Technical Report SCCM-98-01, Department of Computer Science, Stanford University, 1998.

[15] *Matlab User's Guide*, The Math Works, Inc., Natick, MA, 2000